

Controlling magnetic frustration in 1T-TaS₂ via Coulomb engineered long-range interactions

Guangze Chen,¹ Malte Rösner,² and Jose L. Lado¹

¹*Department of Applied Physics, Aalto University, 02150 Espoo, Finland*

²*Institute for Molecules and Materials, Radboud University, NL-6525 AJ Nijmegen, The Netherlands*

(Dated: January 21, 2022)

Magnetic frustrations in two-dimensional materials provide a rich playground to engineer unconventional phenomena such as non-collinear magnetic order and quantum spin-liquid behavior. However, despite intense efforts, a realization of tunable frustrated magnetic order in two-dimensional materials remains an open challenge. Here we propose Coulomb engineering as a versatile strategy to tailor magnetic ground states in layered materials. Using the proximal quantum spin-liquid candidate 1T-TaS₂ as an example, we show how long-range Coulomb interactions renormalize the low energy nearly flat band structure, leading to a Heisenberg model which decisively depends on the Coulomb interactions. Based on this, we show that superexchange couplings in the material can be precisely tailored by means of environmental dielectric screening, ultimately allowing to externally drive the material towards the quantum spin-liquid regime. Our results put forward Coulomb engineering as a powerful tool to manipulate magnetic properties of van der Waals materials.

Magnetic frustration in quantum systems represents one of the fundamental ingredients to stabilize quantum spin-liquid (QSL) physics, characterized by a quantum disordered ground state and fractional excitations[1–5]. Interest in quantum spin-liquids has been fueled by their potential emergent Majorana physics[6], high-temperature superconductivity[7, 8], and use for topological quantum computing[9]. A variety of materials have been proposed as QSL candidates[10–22], yet observing their QSL state is found to be highly sensitive to details of their Hamiltonian. While natural QSL materials are rare and require very precise fine-tuning, engineered materials allow to drastically overcome such challenges. Interestingly, van der Waals QSL candidates such as TaS₂[23–25] and TaSe₂[26] provide versatile platforms for a variety of quantum engineering methods such as straining[27, 28], twisting[29–31], impurity engineering[32–34] as well as Coulomb engineering, that could potentially drive them towards the QSL regime.

Coulomb engineering[35–37] refers to a strategy to tailor many-body interactions by means of dielectric environments, which is particularly efficient for low-dimensional materials. This is due to the pronounced role of non-local Coulomb interactions, which decisively define many-body properties in low-dimensional systems and which can be simultaneously efficiently externally modified. In this way band gaps[37–43] as well as excitonic[37, 42, 44] or plasmonic[45, 46] excitations and even topological properties[47] can be precisely tailored in 2D and 1D systems with the help of (structured) dielectric substrates. Furthermore, Coulomb interactions also play a crucial role in magnetic van der Waals materials, affecting the magnetic exchange between localized magnetic moments. However, up to date, controlling magnetic properties of van der Waals materials via Coulomb engineering has been limited to the example of CrI₃[48].

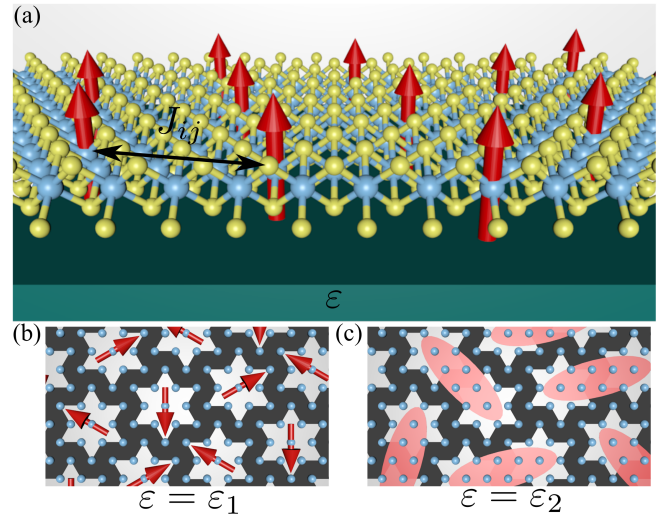


FIG. 1. (a) Sketch of 1T-TaS₂ Coulomb engineered by a substrate with dielectric constant ϵ . The red arrows represent the local magnetic moments in the SOD unit cell. The superexchange couplings J_{ij} between these magnetic moments can be tuned with Coulomb engineering. (b) Sketch of the helical spiral ground state in 1T-TaS₂. The red arrows represent the direction of the local magnetic moment. (c) Sketch of the QSL ground state in 1T-TaS₂.

Here, we put forward Coulomb engineering as a powerful tool to manipulate the ground states of magnetic van der Waals materials, ultimately allowing to stabilize a QSL regime. Using the QSL candidate 1T-TaS₂ as a prototypical example, we show how substrate screening renormalizes its low-energy electronic dispersion and how this controls the internal magnetic superexchange interactions. Together with direct exchange interactions, this allows to externally and non-invasively tailor the magnetic ground state in the material via changes to its dielectric environment. Importantly, beyond the case of

1T-TaS₂ analyzed here, our proposal provides a starting point towards the engineering of artificial magnets via tailored electronic interactions. Ultimately, these results put forward the control of long-range Coulomb interactions as a versatile strategy for quantum matter design.

We now elaborate on the material we will focus on in our discussion, 1T-TaS₂. 1T-TaS₂ hosts a charge-density-wave (CDW) instability leading to the formation of the Star-of-David (SOD) unit cell with 13 atoms at low temperature[23, 49–52]. The CDW as well as spin-orbit coupling (SOC) result in a half-filled narrow band at the Fermi energy, with a bandwidth of a few 10meV[53]. Together with sizable Coulomb interactions[54] this renders 1T-TaS₂ a correlated insulator rather than a simple metal. The electrons form local magnetic moments with $S = 1/2$ at each SOD, and interact via exchange and superexchange coupling (Fig. 1(a)), resulting in potential helical spiral and QSL ground states, as illustrated in Fig. 1(b) and (c), respectively.

We capture the low energy physics of 1T-TaS₂ with a single Wannier orbital model including long-range electronic interactions:

$$H = \sum_{i,j,\sigma} t_{ij} c_{i,\sigma}^\dagger c_{j,\sigma} + U \sum_i n_{i,\uparrow} n_{i,\downarrow} + \sum_{i,j,\sigma,\sigma'} \frac{V_{ij}}{2} n_{i,\sigma} n_{j,\sigma'}, \quad (1)$$

where σ and σ' are spin indices, and $n_{i,\sigma} = c_{i,\sigma}^\dagger c_{i,\sigma}$. The hoppings t_{ij} are fitted to DFT data[54] where we find hoppings up to the 14th neighbour. We parameterize the long-range Coulomb interactions V_{ij} via a modified Yukawa potential of the form

$$V_{ij} = \frac{U}{\sqrt{1 + \left(\frac{4\pi\epsilon_0 U r_{ij}}{e^2}\right)^2}} e^{-r_{ij}/r_{\text{TF}}}, \quad (2)$$

where U is the on-site Coulomb interaction and r_{ij} the distance between sites i and j . The included Ohno potential[43, 55] results in a r^{-1} long-wavelength behaviour, which is further suppressed by the exponential term controlled by an effective screening length r_{TF} . This way, the non-local Coulomb interaction is fully parameterized by the local interaction U and the screening length r_{TF} . It is worth noting that environmental screening to layered materials, such as resulting from dielectric substrates, is strongly non-local[35, 36, 56] such that long-ranged interactions V_{ij} are stronger reduced than the local one U . To fully characterize this model we, however, treat U and r_{TF} as independent parameters in the following, understanding that any environmental screening will reduce both simultaneously.

The interacting model of Eq. (1) is analyzed in two steps. In the limit $U \gg V_{ij}$, we can first integrate out the long-range interactions V_{ij} , leading to a renormalized

dispersion for the low-energy band[57, 58]. The resulting Hamiltonian \tilde{H} takes the form

$$\tilde{H} = \sum_{i,j} \tilde{t}_{ij} c_i^\dagger c_j + U \sum_i n_{i,\uparrow} n_{i,\downarrow}, \quad (3)$$

where \tilde{t}_{ij} are the renormalized hoppings derived from Eq. (1) using a Hatree-Fock variational wavefunction enforcing time-reversal symmetry.

For U between 100 and 500meV as estimated for 1T metallic TMDCs [54, 59] and several choices of r_{TF} the corresponding long-range Coulomb interactions V_n and renormalized hoppings \tilde{t}_n are shown in Figs. 2(a,b), where V_n denotes n^{th} neighbor Coulomb interaction and similarly for \tilde{t}_n . We see that V_n is increased by increasing U and r_{TF} , which mostly affects \tilde{t}_1 for $r_{\text{TF}} < a$ (a is the CDW lattice constant), while the long-range interaction with $r_{\text{TF}} = a$ also modulates hoppings up to \tilde{t}_5 . The corresponding renormalized band structures are shown in Figs. 2(c-f). For $r_{\text{TF}} = 0.3a$ (with $V_{n>1} \approx 0$) the bandwidth is not significantly affected and we find only modifications to the dispersion around Γ upon changing U , c.f. Figs. 2(c,d). Increasing $r_{\text{TF}} > 0.3a$ yields $V_{n>1} > 0$, which decisively affects both, the bandwidth and the overall dispersion, c.f. Figs. 2(e,f). As maintaining the Mott regime requires that the bandwidth renormalization should not be too large, we focus on $r_{\text{TF}} \leq 0.4a$ in the following. In addition to the bandwidth renormalization, we observe a Coulomb controlled Lifshitz transition: as U and r_{TF} increase, the electron pocket at Γ vanishes, as depicted in the insets of Figs. 2(c-f). This transition results in different dependencies of superexchange couplings on the Coulomb interactions as we discuss in the following.

We now analyze the Hamiltonian from Eq. (3) in the strong coupling limit, i.e. $U \gg \tilde{t}_{ij}$, using the Hubbard-Stratonovich transformation, leading to an effective model for spin-degrees of freedom:

$$\mathcal{H} = \sum_{i,j} J_{ij} \mathbf{S}_i \cdot \mathbf{S}_j, \quad (4)$$

with $J_{ij} = 2 \frac{\tilde{t}_{ij}^2}{U}$. Due to the renormalization of t_{ij} by V_{ij} , the magnetic superexchange interactions J_{ij} are controlled by changes to U and r_{TF} as well. This is the first important result of our proposal: Coulomb engineering will control the effective exchange interactions due to their dependence on the local and long-range Coulomb interactions. This key result stems from the renormalization of the band structure, which in the Mott insulating regime of 1T-TaS₂ directly modifies the superexchange interactions. In particular, we show in Fig. 3(a) the renormalized n^{th} neighbor exchange J_n . We see that J_1 exhibits a strong dependence on U and r_{TF} , stemming from the significant renormalization of \tilde{t}_1 . In Fig. 3(b) we depict the full U and r_{TF} dependencies of J_1 in units of $J_1^0 = 0.1\text{meV}$, where J_1^0 is the typical magnitude of J_1 in

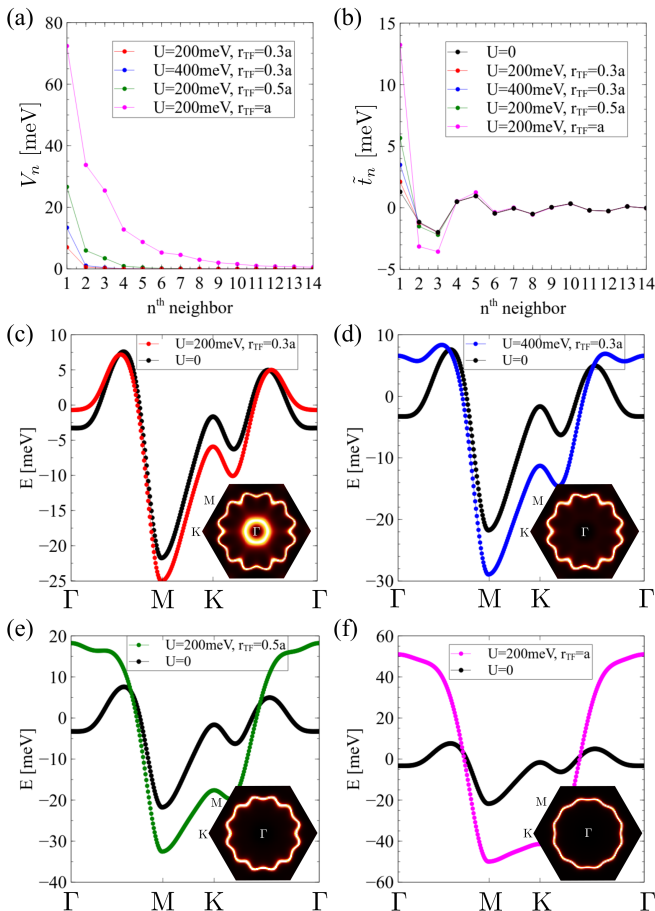


FIG. 2. (a) Long-range Coulomb interactions V_n and (b) the corresponding renormalized hoppings \tilde{t}_n for different values of parameters U and r_{TF} . (c-f) band structure renormalization for different values of U and r_{TF} in (a). The color matches with the color used in (a). The insets show the corresponding Fermi surfaces for the renormalized bands.

our regime. We find two regimes [separated by the white dashed line in Fig. 3(b)] stemming from the Coulomb driven Lifshitz transition of the Hamiltonian of Eq. (1). In the upper regime V_n has a long-range character yielding renormalized band structures with unoccupied and rather flat dispersions around Γ , while in the lower regime the Coulomb interaction is short-ranged (U and V_1) and we find occupied electron pockets (with positive effective mass) around Γ . J_1 is correspondingly larger in the upper regime and strongly dependent on r_{TF} . In the lower regime J_1 is reduced and mostly dependent on U .

We note that the Heisenberg model Eq. (4) includes only superexchange couplings stemming from the local repulsion. Apart from that, it is important to note that direct exchange stemming from the overlap of Wannier centers would also appear in the effective Heisenberg model[54, 60]. In particular, strong direct exchange interactions promote a ferromagnetic ground state in 1T-TaS₂[54]. To account for this, we now include the direct

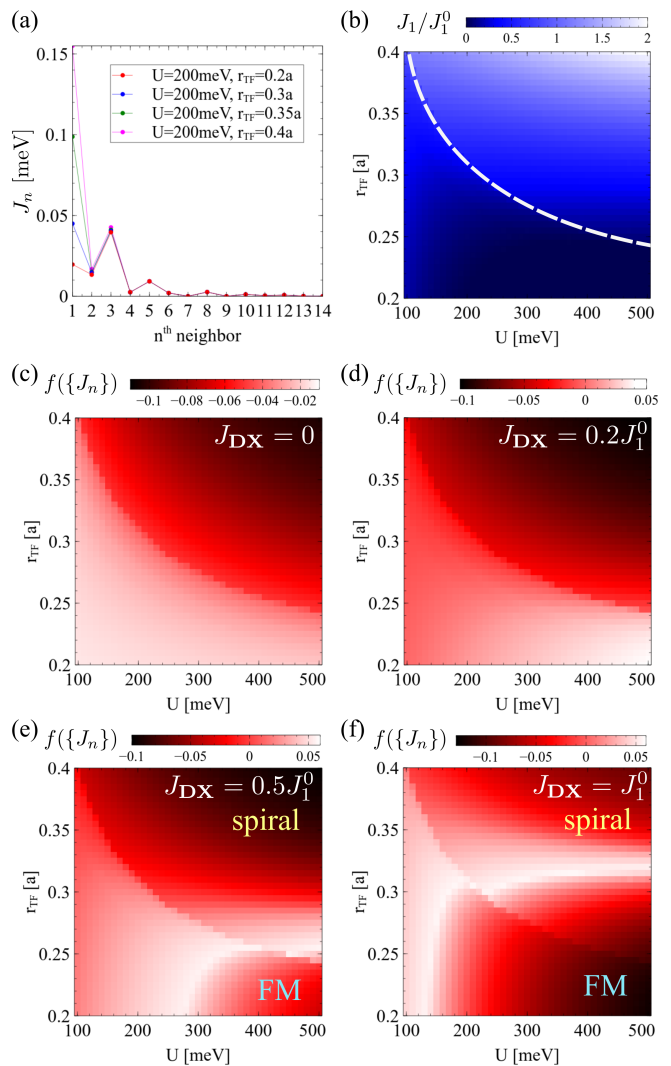


FIG. 3. (a) Long-range spin superexchange couplings J_n for different values of U and r_{TF} . Only J_1 is significantly influenced by U and r_{TF} . (b) J_1 for different values of U and r_{TF} , in units of $J_1^0 = 0.1\text{meV}$. The dashed line indicates a discontinuity stemming from the Lifshitz transition. (c-f) Frustration index for the model of Eq. (5) as a function of U and r_{TF} , with (c) $J_{\text{DX}} = 0$, (d) $J_{\text{DX}} = 0.2J_1^0$, (e) $J_{\text{DX}} = 0.5J_1^0$ and (f) $J_{\text{DX}} = J_1^0$.

exchange term in the Heisenberg model, which results from Hund's exchange interaction and can thus be assumed to be independent on the environmental screening [48]. The corresponding Heisenberg model reads

$$\mathcal{H} = \sum_{i,j} J_{ij} \mathbf{S}_i \cdot \mathbf{S}_j + J_{\text{DX}} \sum_{\langle i,j \rangle} \mathbf{S}_i \cdot \mathbf{S}_j, \quad (5)$$

where J_{DX} is the magnitude of first neighbor direct exchange. When the superexchange is small, the system is dominated by the direct exchange J_{DX} yielding a ferromagnetic ground state. When the first neighbor superexchange dominates over the direct exchange, the system

exhibits a helical spiral state[61] due to the large antiferromagnetic J_1 . In the intermediate regime, the competition between J_{ij} and J_{DX} leads to a state dominated by long-range antiferromagnetic coupling, potentially leading to a QSL ground state.

The model of Eq. (5) thus realizes a long-range Heisenberg model with tunable frustration controlled by the local and non-local Coulomb interactions. While a full calculation of the phase diagram would require to exactly solve the two-dimensional quantum many-body model, e.g. with tensor-network[62, 63] or neural network quantum states[64, 65], here we will focus on highlighting the physical regime where the frustration of the system is maximal. Focusing on the ferromagnetic and antiferromagnetic phases mentioned above, we quantitatively capture the frustration of the spin model by introducing a frustration index $f(\{J_n\})$ defined as:

$$f(\{J_n\}) = \frac{\min(E_{\text{helical}}, E_{\text{FM}})}{\mathcal{J}}, \quad (6)$$

where E_{helical} is the energy of the helical spiral state, E_{FM} is the energy of the ferromagnetic phase, and $\mathcal{J} = \sum_{i,j} |J_{ij}|$ is the energy normalization factor. The larger the frustration index, the higher energy the two classical ground states have in comparison with the whole manifold of states, therefore giving rise to the possibility of a lower energy QSL ground state to emerge. The frustration index defined above can be generalized to include other potential classical ground states of a Heisenberg model, such as the stripe phase[66] which would appear for dominating antiferromagnetic J_2 . As an outlook, we note that a more sophisticated description of the frustration can be performed by exactly solving the many-body system and analyzing the mathematical structure of the associated reduced density matrices[67]. We finally note that while the frustration index does not provide an exact mapping of the phase diagram, it allows to efficiently pinpoint the regions of the phase diagram where competing QSL may appear.

To characterize the competition between magnetic phases, we show in Figs. 3(c-f) the frustration index for the full model using different J_{DX} in the U/r_{TF} plane. When $J_{\text{DX}} = 0$, as shown in Fig. 3(c), the spiral ground state dominates the whole parameter space and the frustration index monotonically decreases with U and r_{TF} . In this case the QSL regime would be favored for small U and r_{TF} as resulting from increased environmental screening. We note that the discontinuity discussed above is also visible here. For $J_{\text{DX}} = 0.2J_1^0$, shown in Fig. 3(d), the frustration index is enhanced (and thus the possibility to drive the system into the QSL phase) for small r_{TF} and large U . More interestingly, when $J_{\text{DX}} \geq 0.2J_1^0$, as shown in Fig. 3(e) and (f), we find both, the spiral and FM phases in the phase diagrams. This feature highlights that Coulomb engineering can be utilized to switch between these classical magnetic

ground states. Even more promising is the border between these ground states as we find here the maximal degree of frustration, which defines a "sweet spot" for the stabilization of the QSL regime. Finally, for larger J_{DX} the ferromagnetic ground state would dominate the whole parameter space. Hence, for small J_{DX} strong environmental screening is most beneficial to drive the system toward the QSL regime, while for $J_{\text{DX}} \geq 0.2J_1^0$ the optimal environmental screening for the stabilization of the QSL phase depends on J_{DX} . For both cases, we however clearly see the potential of Coulomb engineering to tailor the magnetic ground state. In practice this can be achieved by exposing the monolayer to different substrates, such as SiO_2 , SrTiO_3 , or hBN, or by embedding it in a tunable dielectric environment[68, 69].

Finally, we comment on several aspects that should be addressed in future work. First, our analysis focuses on a spin-isotropic model, where potentially anisotropic terms stemming from spin-orbit coupling are not included. The inclusion of spin-orbit coupling in the low-energy model would give rise to spin-dependent hoppings, which in turn could induce anisotropic exchange in the spin model generating an even richer phase diagram. Second, we used a Hatree-Fock variational wavefunction to capture the bandwidth renormalization induced by V_{ij} , while a more accurate approach would be extensions of the Peierls-Feynman-Bogoliubov variational principle [57, 70, 71] taking the full non-local Coulomb and nearest neighbour exchange interactions into account. Yet for long-range V_{ij} up to 3rd neighbor, such an approach involves heavy computation that would go beyond the scope of this work. Third, although we used the 1T-TaS₂ band structure as an example here, the same methodology can be applied to other van der Waals materials such as 1T-NbSe₂[59, 72–74], 1T-NbS₂[75], 1T-TaSe₂[76], as well as other 1T-dichalcogenide alloys, and potentially twisted graphene multilayers[77, 78], driving them to exotic magnetic phases. As an outlook, Coulomb engineering can also be performed with spatially structured[37, 38, 41, 46, 47] or anisotropic[79, 80] screening environments giving rise to spatially dependent exchange interactions, that potentially leads to coexisting ground states of different character within the same, homogeneous layered material.

To summarize, we have put forward a strategy to control the magnetic ground state of strongly correlated layered materials, which shows the potential to drive a two-dimensional magnetic material to a frustrated quantum spin-liquid regime by means of Coulomb engineering. Taking as a starting point the Wannier model for the nearly flat band structure in 1T-TaS₂, we demonstrated that tunable screening drastically impacts the low-energy spin model of the system. In particular, we showed that the long-range Coulomb interactions result in bandwidth renormalization at the Hatree-Fock level. The renormalized bandwidth, together with the long-range nature of

the Wannier model gives rise in the strongly interacting limit to a screening-dependent frustrated Heisenberg model. Finally, we showed how tuning the long-range Coulomb interaction via screening can bring the system towards the QSL regime by analyzing the frustration of the spin system. Our proposal demonstrates how substrate-dependent screening, widely present in studies of van der Waals heterostructures, provides a powerful strategy to stabilize unconventional correlated states of matter. Ultimately, our results provide a starting point towards tailoring frustrated quantum magnetism via Coulomb engineering, potentially allowing to stabilize quantum spin-liquid physics in a variety of van der Waals magnets.

Acknowledgements We acknowledge the computational resources provided by the Aalto Science-IT project, and the financial support from the Academy of Finland Projects No. 331342 and No. 336243. We thank M. I. Katsnelson, A. N. Rudenko, A. A. Bagrov, T. Westerhout, P. Liljeroth and V. Vaño for fruitful discussions.

-
- [1] L. Balents, *Nature* **464**, 199 (2010).
- [2] P. A. Lee, *Science* **321**, 1306 (2008).
- [3] C. Broholm, R. J. Cava, S. A. Kivelson, D. G. Nocera, M. R. Norman, and T. Senthil, *Science* **367**, eaay0668 (2020).
- [4] Y. Zhou, K. Kanoda, and T.-K. Ng, *Rev. Mod. Phys.* **89**, 025003 (2017).
- [5] L. Savary and L. Balents, *Reports on Progress in Physics* **80**, 016502 (2016).
- [6] A. Kitaev, *Annals of Physics* **321**, 2 (2006).
- [7] P. W. Anderson, *Science* **235**, 1196 (1987).
- [8] Z. A. Kelly, M. J. Gallagher, and T. M. McQueen, *Phys. Rev. X* **6**, 041007 (2016).
- [9] D. Aasen, R. S. K. Mong, B. M. Hunt, D. Mandrus, and J. Alicea, *Phys. Rev. X* **10**, 031014 (2020).
- [10] T.-H. Han, J. S. Helton, S. Chu, D. G. Nocera, J. A. Rodriguez-Rivera, C. Broholm, and Y. S. Lee, *Nature* **492**, 406 (2012).
- [11] M. Fu, T. Imai, T.-H. Han, and Y. S. Lee, *Science* **350**, 655 (2015).
- [12] B. J. Powell and R. H. McKenzie, *Reports on Progress in Physics* **74**, 056501 (2011).
- [13] S. K. Takahashi, J. Wang, A. Arsenault, T. Imai, M. Abramchuk, F. Tafti, and P. M. Singer, *Phys. Rev. X* **9**, 031047 (2019).
- [14] M. R. Norman, *Rev. Mod. Phys.* **88**, 041002 (2016).
- [15] H. Takagi, T. Takayama, G. Jackeli, G. Khaliullin, and S. E. Nagler, *Nature Reviews Physics* **1**, 264 (2019).
- [16] Y. Shimizu, K. Miyagawa, K. Kanoda, M. Maesato, and G. Saito, *Phys. Rev. Lett.* **91**, 107001 (2003).
- [17] M. Yamashita, N. Nakata, Y. Kasahara, T. Sasaki, N. Yoneyama, N. Kobayashi, S. Fujimoto, T. Shibauchi, and Y. Matsuda, *Nature Physics* **5**, 44 (2008).
- [18] T. Itou, A. Oyamada, S. Maegawa, M. Tamura, and R. Kato, *Phys. Rev. B* **77**, 104413 (2008).
- [19] T. Isono, H. Kamo, A. Ueda, K. Takahashi, M. Kimata, H. Tajima, S. Tsuchiya, T. Terashima, S. Uji, and H. Mori, *Phys. Rev. Lett.* **112**, 177201 (2014).
- [20] J. S. Helton, K. Matan, M. P. Shores, E. A. Nytko, B. M. Bartlett, Y. Yoshida, Y. Takano, A. Suslov, Y. Qiu, J.-H. Chung, D. G. Nocera, and Y. S. Lee, *Phys. Rev. Lett.* **98**, 107204 (2007).
- [21] L. Ding, P. Manuel, S. Bachus, F. Grüfler, P. Gegenwart, J. Singleton, R. D. Johnson, H. C. Walker, D. T. Adroja, A. D. Hillier, and A. A. Tsirlin, *Phys. Rev. B* **100**, 144432 (2019).
- [22] M. M. Bordelon, E. Kenney, C. Liu, T. Hogan, L. Posthuma, M. Kavand, Y. Lyu, M. Sherwin, N. P. Butch, C. Brown, M. J. Graf, L. Balents, and S. D. Wilson, *Nature Physics* **15**, 1058 (2019).
- [23] K. T. Law and P. A. Lee, *Proceedings of the National Academy of Sciences* **114**, 6996 (2017).
- [24] H. Murayama, Y. Sato, T. Taniguchi, R. Kurihara, X. Z. Xing, W. Huang, S. Kasahara, Y. Kasahara, I. Kimchi, M. Yoshida, Y. Iwasa, Y. Mizukami, T. Shibauchi, M. Konczykowski, and Y. Matsuda, *Phys. Rev. Research* **2**, 013099 (2020).
- [25] S. Mañas-Valero, B. Huddart, T. Lancaster, E. Coronado, and F. Pratt, arXiv e-prints, arXiv:2007.15905 (2020), arXiv:2007.15905 [cond-mat.str-el].
- [26] Y. Chen, W. Ruan, M. Wu, S. Tang, H. Ryu, H.-Z. Tsai, R. Lee, S. Kahn, F. Liou, C. Jia, O. R. Albertini, H. Xiong, T. Jia, Z. Liu, J. A. Sobota, A. Y. Liu, J. E. Moore, Z.-X. Shen, S. G. Louie, S.-K. Mo, and M. F. Crommie, *Nature Physics* **16**, 218 (2020).
- [27] F. Guinea, M. I. Katsnelson, and A. K. Geim, *Nature Physics* **6**, 30 (2009).
- [28] C. Xu, J. Feng, M. Kawamura, Y. Yamaji, Y. Nahas, S. Prokhorenko, Y. Qi, H. Xiang, and L. Bellaiche, *Phys. Rev. Lett.* **124**, 087205 (2020).
- [29] J. M. B. Lopes dos Santos, N. M. R. Peres, and A. H. Castro Neto, *Phys. Rev. Lett.* **99**, 256802 (2007).
- [30] E. Y. Andrei, D. K. Efetov, P. Jarillo-Herrero, A. H. MacDonald, K. F. Mak, T. Senthil, E. Tutuc, A. Yazdani, and A. F. Young, *Nature Reviews Materials* **6**, 201–206 (2021).
- [31] G. Chen and J. L. Lado, *Phys. Rev. Research* **3**, 033276 (2021).
- [32] H. Gonzalez-Herrero, J. M. Gomez-Rodriguez, P. Mallet, M. Moaied, J. J. Palacios, C. Salgado, M. M. Ugeda, J.-Y. Veuillen, F. Yndurain, and I. Brihuega, *Science* **352**, 437 (2016).
- [33] L. Savary and L. Balents, *Phys. Rev. Lett.* **118**, 087203 (2017).
- [34] G. Chen and J. L. Lado, *Phys. Rev. Research* **2**, 033466 (2020).
- [35] D. Jena and A. Konar, *Phys. Rev. Lett.* **98**, 136805 (2007).
- [36] M. Rösner, E. Şaşıoğlu, C. Friedrich, S. Blügel, and T. O. Wehling, *Phys. Rev. B* **92**, 085102 (2015).
- [37] A. Raja, A. Chaves, J. Yu, G. Arefe, H. M. Hill, A. F. Rigosi, T. C. Berkelbach, P. Nagler, C. Schüller, T. Korn, C. Nuckolls, J. Hone, L. E. Brus, T. F. Heinz, D. R. Reichman, and A. Chernikov, *Nature Communications* **8** (2017), 10.1038/ncomms15251.
- [38] M. Rösner, C. Steinke, M. Lorke, C. Gies, F. Jahnke, and T. O. Wehling, *Nano Letters* **16**, 2322 (2016).
- [39] A. Steinhoff, M. Florian, M. Rösner, G. Schönhoff, T. O. Wehling, and F. Jahnke, *Nature Communications* **8**, 1166 (2017).
- [40] M. I. B. Utama, H. Kleemann, W. Zhao, C. S. Ong,

- F. H. da Jornada, D. Y. Qiu, H. Cai, H. Li, R. Kou, S. Zhao, S. Wang, K. Watanabe, T. Taniguchi, S. Tongay, A. Zettl, S. G. Louie, and F. Wang, *Nature Electronics* **2**, 60 (2019).
- [41] C. Steinke, T. O. Wehling, and M. Rösner, *Phys. Rev. B* **102**, 115111 (2020).
- [42] L. Waldecker, A. Raja, M. Rösner, C. Steinke, A. Bostwick, R. J. Koch, C. Jozwiak, T. Taniguchi, K. Watanabe, E. Rotenberg, T. O. Wehling, and T. F. Heinz, *Phys. Rev. Lett.* **123**, 206403 (2019).
- [43] E. G. C. P. van Loon, M. Schüler, D. Springer, G. Sangiovanni, J. M. Tomczak, and T. O. Wehling, “Coulomb engineering of two-dimensional mott materials,” (2020), [arXiv:2001.01735 \[cond-mat.str-el\]](https://arxiv.org/abs/2001.01735).
- [44] C. Steinke, D. Mourad, M. Rösner, M. Lorke, C. Gies, F. Jahnke, G. Czycholl, and T. O. Wehling, *Phys. Rev. B* **96**, 045431 (2017).
- [45] F. H. da Jornada, L. Xian, A. Rubio, and S. G. Louie, *Nature Communications* **11**, 1013 (2020).
- [46] Z. Jiang, S. Haas, and M. Rösner, *2D Materials* **8**, 035037 (2021).
- [47] M. Rösner and J. L. Lado, *Phys. Rev. Research* **3**, 013265 (2021).
- [48] D. Soriano, A. N. Rudenko, M. I. Katsnelson, and M. Rösner, *npj Computational Materials* **7** (2021), [10.1038/s41524-021-00631-4](https://doi.org/10.1038/s41524-021-00631-4).
- [49] D. Cho, S. Cheon, K.-S. Kim, S.-H. Lee, Y.-H. Cho, S.-W. Cheong, and H. W. Yeom, *Nature Communications* **7** (2016), [10.1038/ncomms10453](https://doi.org/10.1038/ncomms10453).
- [50] S. Qiao, X. Li, N. Wang, W. Ruan, C. Ye, P. Cai, Z. Hao, H. Yao, X. Chen, J. Wu, Y. Wang, and Z. Liu, *Phys. Rev. X* **7**, 041054 (2017).
- [51] M. Kratochvilova, A. D. Hillier, A. R. Wildes, L. Wang, S.-W. Cheong, and J.-G. Park, *npj Quantum Mater.* **2**, 42 (2017).
- [52] V. Vaño, M. Amini, S. C. Ganguli, G. Chen, J. L. Lado, S. Kezilebieke, and P. Liljeroth, *Nature* **599**, 582–586 (2021).
- [53] K. Rossnagel and N. V. Smith, *Phys. Rev. B* **73**, 073106 (2006).
- [54] D. Pasquier and O. V. Yazyev, *arXiv e-prints*, [arXiv:2108.11277](https://arxiv.org/abs/2108.11277) (2021), [arXiv:2108.11277 \[cond-mat.mtrl-sci\]](https://arxiv.org/abs/2108.11277).
- [55] K. Ohno, *Theoretica chimica acta* **2**, 219 (1964).
- [56] L. V. Keldysh, *Pis'ma Zh. Eksp. Teor. Fiz.* **29**, 716 (1979).
- [57] Y. in 't Veld, M. Schüler, T. O. Wehling, M. I. Katsnelson, and E. G. C. P. van Loon, *Journal of Physics: Condensed Matter* **31**, 465603 (2019).
- [58] T. Ayrál, S. Biermann, P. Werner, and L. Boehnke, *Phys. Rev. B* **95**, 245130 (2017).
- [59] E. Kamil, J. Berges, G. Schönhoff, M. Rösner, M. Schüler, G. Sangiovanni, and T. O. Wehling, *Journal of Physics: Condensed Matter* **30**, 325601 (2018).
- [60] V. V. Mazurenko, A. N. Rudenko, S. A. Nikolaev, D. S. Medvedeva, A. I. Lichtenstein, and M. I. Katsnelson, *Phys. Rev. B* **94**, 214411 (2016).
- [61] P. Fazekas and P. W. Anderson, *Philosophical Magazine* **30**, 423 (1974).
- [62] S. Yan, D. A. Huse, and S. R. White, *Science* **332**, 1173 (2011).
- [63] S. Hu, W. Zhu, S. Eggert, and Y.-C. He, *Phys. Rev. Lett.* **123**, 207203 (2019).
- [64] G. Carleo and M. Troyer, *Science* **355**, 602 (2017).
- [65] K. Choo, T. Neupert, and G. Carleo, *Phys. Rev. B* **100**, 125124 (2019).
- [66] T. Jolicoeur, E. Dagotto, E. Gagliano, and S. Bacci, *Phys. Rev. B* **42**, 4800 (1990).
- [67] S. M. Giampaolo, G. Gualdi, A. Monras, and F. Illuminati, *Phys. Rev. Lett.* **107**, 260602 (2011).
- [68] A. C. Riis-Jensen, J. Lu, and K. S. Thygesen, *Phys. Rev. B* **101**, 121110 (2020).
- [69] Y. Saito, J. Ge, K. Watanabe, T. Taniguchi, and A. F. Young, *Nature Physics* **16**, 926 (2020).
- [70] M. Schüler, M. Rösner, T. O. Wehling, A. I. Lichtenstein, and M. I. Katsnelson, *Phys. Rev. Lett.* **111**, 036601 (2013).
- [71] E. G. C. P. van Loon, M. Schüler, M. I. Katsnelson, and T. O. Wehling, *Phys. Rev. B* **94**, 165141 (2016).
- [72] D. Pasquier and O. V. Yazyev, *Phys. Rev. B* **98**, 045114 (2018).
- [73] Y. Nakata, K. Sugawara, R. Shimizu, Y. Okada, P. Han, T. Hitosugi, K. Ueno, T. Sato, and T. Takahashi, *NPG Asia Materials* **8**, e321 (2016).
- [74] M. Liu, J. Leveillee, S. Lu, J. Yu, H. Kim, C. Tian, Y. Shi, K. Lai, C. Zhang, F. Giustino, and C.-K. Shih, *Science Advances* **7** (2021), [10.1126/sciadv.abi6339](https://doi.org/10.1126/sciadv.abi6339).
- [75] W. Wang, B. Wang, Z. Gao, G. Tang, W. Lei, X. Zheng, H. Li, X. Ming, and C. Autieri, *Phys. Rev. B* **102**, 155115 (2020).
- [76] W. Ruan, Y. Chen, S. Tang, J. Hwang, H.-Z. Tsai, R. L. Lee, M. Wu, H. Ryu, S. Kahn, F. Liou, C. Jia, A. Aikawa, C. Hwang, F. Wang, Y. Choi, S. G. Louie, P. A. Lee, Z.-X. Shen, S.-K. Mo, and M. F. Crommie, *Nature Physics* **17**, 1154 (2021).
- [77] J. M. Pizarro, M. Rösner, R. Thomale, R. Valentí, and T. O. Wehling, *Phys. Rev. B* **100**, 161102 (2019).
- [78] T. M. R. Wolf, J. L. Lado, G. Blatter, and O. Zilberberg, *Phys. Rev. Lett.* **123**, 096802 (2019).
- [79] F. Xia, H. Wang, and Y. Jia, *Nature Communications* **5** (2014), [10.1038/ncomms5458](https://doi.org/10.1038/ncomms5458).
- [80] B. Kiraly, E. J. Knol, K. Volckaert, D. Biswas, A. N. Rudenko, D. A. Prishchenko, V. G. Mazurenko, M. I. Katsnelson, P. Hofmann, D. Wegner, and A. A. Khajetoorians, *Phys. Rev. Lett.* **123**, 216403 (2019).